Title

Mechanisms by which sialylated milk oligosaccharides impact bone biology in a gnotobiotic mouse model of infant undernutrition

Journal

Proceedings of the National Academy of Sciences of the United States of America, 116(24)

ISSN

0027-8424

Authors

Cowardin, Carrie A
Ahern, Philip P
Kung, Vanderlene L
et al.

Publication Date

2019-06-11

DOI

10.1073/pnas.1821770116

Peer reviewed

Mechanisms by which sialylated milk oligosaccharides impact bone biology in a gnotobiotic mouse model of infant undernutrition

Carrie A. Cowardin[a,b], Philip P. Ahern[a,b], Vanderlene L. Kung[a,b], Matthew C. Hibberd[a,b], Jiye Cheng[a,b], Janaki L. Guruge[a,b], Vinaik Sundaresan[a,b], Richard D. Head[c,d], Daniela Barile[e,f], David A. Mills[e,f], Michael J. Barratt[a,b], Sayeeda Huq[g], Tahmeed Ahmed[g], and Jeffrey I. Gordon[a,b,1]

[a]Edison Family Center for Genome Sciences and Systems Biology, Washington University School of Medicine, St. Louis, MO 63110; [b]Center for Gut Microbiome and Nutrition Research, Washington University School of Medicine, St. Louis, MO 63110; [c]Department of Genetics, Washington University School of Medicine, St. Louis, MO 63110; [d]Genome Technology Access Center, Washington University School of Medicine, St. Louis, MO 63110; [e]Foods for Health Institute, University of California, Davis, CA 95616; [f]Department of Food Science and Technology, University of California, Davis, CA 95616; and [g]International Centre for Diarrhoeal Disease Research, 1212 Dhaka, Bangladesh

Contributed by Jeffrey I. Gordon, April 10, 2019 (sent for review December 24, 2018; reviewed by Martin J. Blaser and Sharon M. Donovan)

Undernutrition in children is a pressing global health problem, manifested in part by impaired linear growth (stunting). Current nutritional interventions have been largely ineffective in overcoming stunting, emphasizing the need to obtain better understanding of its underlying causes. Treating Bangladeshi children with severe acute malnutrition with therapeutic foods reduced plasma levels of a biomarker of osteoclastic activity without affecting biomarkers of osteoblastic activity or improving their severe stunting. To characterize interactions among the gut microbiota, human milk oligosaccharides (HMOs), and osteoclast and osteoblast biology, young germ-free mice were colonized with cultured bacterial strains from a 6-mo-old stunted infant and fed a diet mimicking that consumed by the donor population. Adding purified bovine sialylated milk oligosaccharides (S-BMO) with structures similar to those in human milk to this diet increased femoral trabecular bone volume and cortical thickness, reduced osteoclasts and their bone marrow progenitors, and altered regulators of osteoclastogenesis and mediators of Th2 responses. Comparisons of germ-free and colonized mice revealed S-BMO-dependent and microbiota-dependent increases in cecal levels of succinate, increased numbers of small intestinal tuft cells, and evidence for activation of a succinate-induced tuft cell signaling pathway linked to Th2 immune responses. A prominent fucosylated HMO, 2′-fucosyllactose, failed to elicit these changes in bone biology, highlighting the structural specificity of the S-BMO effects. These results underscore the need to further characterize the balance between, and determinants of, osteoclastic and osteoblastic activity in stunted infants/children, and suggest that certain milk oligosaccharides may have therapeutic utility in this setting.

childhood undernutrition | stunting | gut microbiota | bone growth | breast milk oligosaccharides

Undernutrition is a pressing global health challenge, annually contributing to the deaths of more than 3 million children younger than 5 y (1). Infants and children whose length-for-age z-score (LAZ) is at least two SDs below the median of the World Health Organization's Child Growth Standard (LAZ <−2) are defined as stunted. Efforts to reduce stunting through nutritional interventions have been largely ineffective (2). Moreover, the long-term sequelae of stunting, including poor vaccine responses, complications in pregnancy, reduced cognitive ability, and loss of economic productivity, contribute to the intergenerational cycle of undernutrition (3, 4). Numerous factors, ranging from micronutrient deficiencies to enteropathogen exposure, systemic inflammation, and host genetic/epigenetic features, have been invoked to explain stunting in undernourished children (5–7). However, a more comprehensive molecular characterization of the biological state of children with undernutrition is needed to ascertain the mechanisms underlying linear growth faltering, to understand why current treatments fail, and to develop new interventions with significantly greater efficacy.

In the present report, we examine interactions among milk oligosaccharides, osteoclast and osteoblast biology, and components of the immune system to gain insights about the pathogenesis of stunting. Our rationale for examining these interactions are as follows. First, there is little information about how stunting correlates with the number and activity of myeloid-derived osteoclasts that degrade bone surface and osteoblasts that produce new bone. Second, the immune system plays a major role in the differentiation

Significance

Identifying components of breast milk that influence postnatal development though their effects on the gut microbiota and immune system could provide new therapeutic approaches for childhood undernutrition, including heretofore treatment-refractory linear growth faltering (stunting). Plasma biomarkers of osteoclast-mediated bone resorption and osteoblast-driven bone formation in stunted Bangladeshi children provided evidence for elevated osteoclastic activity. Gnotobiotic mice, colonized with a stunted infant's gut microbiota, exhibited decreased bone resorption when consuming diets supplemented with a purified bovine oligosaccharide mixture dominated by sialylated structures found in human breast milk. Supplementation decreased osteoclastogenesis while sparing osteoblast activity; the microbiota, intestinal cell populations, and immune mediators contribute to these responses. The influence of milk oligosaccharides on the gut microbiota–bone axis has diagnostic and therapeutic implications.

Author contributions: C.A.C., M.J.B., S.H., T.A., and J.I.G. designed research; C.A.C., P.P.A., V.L.K., J.C., J.L.G., S.H., and T.A. performed research; R.D.H., D.B., and D.A.M. contributed new reagents/analytic tools; C.A.C., P.P.A., V.L.K., M.C.H., J.C., V.S., M.J.B., and J.I.G. analyzed data; and C.A.C., M.J.B., and J.I.G. wrote the paper.

Reviewers: M.J.B., NYU Langone Medical Center; and S.M.D., University of Illinois.

Conflict of interest statement: D.B. and D.A.M. are cofounders of Evolve Biosystems, a company focused on diet-based manipulation of the gut microbiota. J.I.G. is a cofounder of Matatu, Inc., a company characterizing the role of diet-by-microbiota interactions in animal health.

Data deposition: COPRO-Seq and RNA-Seq datasets, plus genome assemblies of infant gut bacterial strains, have been deposited at the European Nucleotide Archive under study accession no. PRJEB29697 (see PRJEB9488 for shotgun sequencing datasets of the bacterial genomes).

[1]To whom correspondence should be addressed. Email: jgordon@wustl.edu.

This article contains supporting information online at www.pnas.org/lookup/suppl/doi:10.1073/pnas.1821770116/-/DCSupplemental.

Published online May 28, 2019.

of both the osteoclast and osteoblast lineages and in regulating their function (8–10). Insulin-like growth factor-1 (IGF1) is a key effector in the growth hormone signaling pathway that influences bone growth and other facets of postnatal development. Proinflammatory cytokines, such as IL-6, TNFα, and IL-1β, can reduce growth hormone (GH) receptor levels in liver and in the growth plates of bones; they also impair GH signaling via suppressor of cytokine signaling (SOCS)-mediated inhibition of JAK2 and STAT activity (11), leading to impaired responsiveness to IGF1. In addition to their effects on IGF1 activity, proinflammatory cytokines can affect bone production through effects on PI3K/Akt2 and JAK/STAT3 signaling pathways that control survival and differentiation of osteoblasts (12). A similar relationship between systemic inflammation and impaired GH/IGF1 signaling has been implicated in the linear growth deficiency that develops in children with inflammatory bowel disease (13–15) and chronic renal failure (16). Third, human milk oligosaccharides (HMOs) are branched or linear structures composed of glucose, galactose, and *N*-acetylglucosamine residues that can be decorated with fucose or sialic acid in a number of linkage configurations. A study of two Malawian birth cohorts disclosed that sialylated milk oligosaccharides were significantly less abundant in mothers with severely stunted infants (17). Preclinical evidence of a connection between HMOs and bone growth was provided by studies of young gnotobiotic mice colonized with a consortium of bacterial strains cultured from the fecal microbiota of a 6-mo-old stunted Malawian infant (17). Mice were fed a prototypic Malawian diet with or without sialylated milk oligosaccharide structures purified from bovine milk (S-BMO) that are also present in human breast milk. Microcomputed tomography of their femurs disclosed that S-BMO supplementation was associated with significant increases in the volume of trabecular bone, as well as cortical bone (17).

In the current study, we show that a cohort of stunted children with severe acute malnutrition (SAM) exhibit increased osteoclastic activity before therapeutic food intervention, without effects on osteoblastic activity. We use gnotobiotic mice to demonstrate how S-BMO produces effects on bone growth through selective reductions in osteoclastogenesis, while sparing osteoblast activity. These effects are not evident in colonized mice treated with 2′-fucosyllactose (2′-FL), a representative of the structurally diverse and prominent fucosylated oligosaccharides present in breast milk. Our results identify interactions between milk oligosaccharides and the gut microbiota that provide potential new therapeutic targets for overcoming the heretofore intractable problem of stunting in undernourished children.

Results

Assessing Osteoclastic and Osteoblastic Activity in Children with Severe Acute Malnutrition. A cohort of Bangladeshi children with SAM (weight-for-height Z-score < −3) were enrolled in a randomized, double-blind study to compare the efficacy of two locally produced, ready-to-use therapeutic foods and a commercially available ready-to-use therapeutic food on the rate of weight gain after subjects had first been stabilized, using a hospital-based, standardized management protocol for SAM (18). After initial stabilization, children were randomly assigned into one of the three treatment groups and provided ∼200 kcal of the ready-to-use therapeutic food/kg/d until they had achieved an edema-free weight-for-height Z-score of at least −2, at which time they were discharged from the hospital. A subcohort of 54 children aged 17 ± 7.5 (mean ± SD) mo at enrollment was followed at regular intervals up to 12 mo after discharge, with blood samples obtained at enrollment, after completing treatment (mean duration, 16 d) and 6 mo postdischarge. Linear growth was assessed by anthropometry monthly for 6 mo. Despite their positive effects on short-term weight gain, none of the interventions resulted in a significant improvement in their severe stunting [LAZ; −3.32 ± 1.47 (mean ± SD) at enrollment, −3.31 ± 1.32 after 6 mo postdischarge; $P = 0.97$, Wilcoxon matched-pairs signed rank test].

We used plasma samples serially collected from these children before and after treatment to measure biomarkers and regulators of bone turnover. The results revealed that C-Terminal Telopeptide of Type I Collagen (CTX-I), a biomarker released during osteoclastic bone degradation (19), decreased significantly after nutritional therapy (Fig. 1*A*). IL-6 and TNFα, both known pro-osteoclastogenic cytokines (20, 21), also decreased significantly 6 mo after therapy, as did C-reactive protein (CRP), an acute-phase reactant that can increase osteoclast numbers (Fig. 1 *B–D*). In contrast, Pro-Collagen Type I Propeptide (P1NP), a marker of osteoblastic bone production, did not change (Fig. 1*E*). We concluded that although the nutritional interventions did not significantly change LAZ scores, they altered levels of CTX-I and inflammatory mediators in ways that would be anticipated to reduce osteoclast number/activity.

S-BMO Diminishes Bone Resorption in Gnotobiotic Mice Colonized with Gut Bacteria from a Stunted 6-Mo-Old Infant. On the basis of these findings, we turned to the gnotobiotic mouse model described in the Introduction to examine whether S-BMO affects the balance between osteoclast and osteoblast number and activity. Dietary information obtained from Malawian infants during the period of complementary feeding was used to generate a representative diet consisting of eight principal ingredients

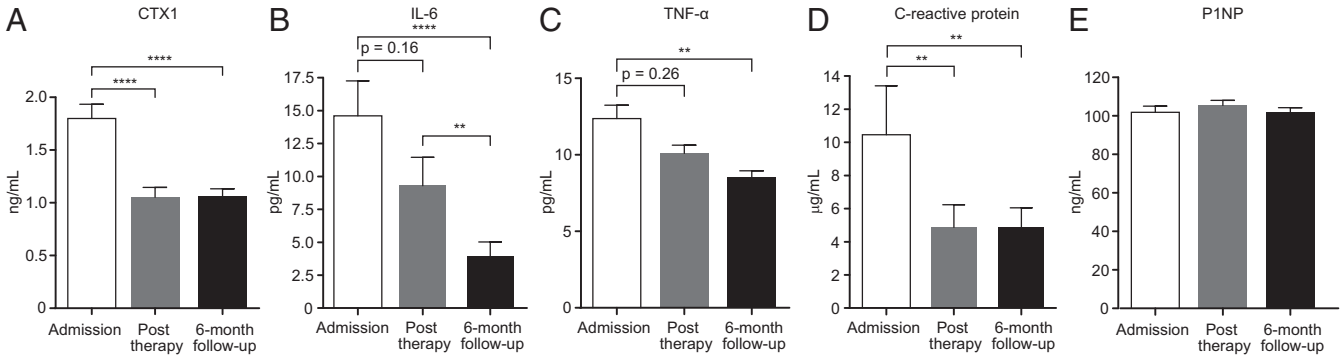

Fig. 1. Characterization of bone and immune biomarkers in Bangladeshi children with SAM before and after nutritional intervention. Plasma samples were obtained before treatment, immediately after treatment, and at 6 mo follow-up ($n = 40$–49 samples/analyte). Mean values ± SEM are plotted for CTX-I (*A*), IL-6 (*B*), TNFα (*C*), CRP (*D*), and P1NP (*E*). *$P < 0.05$; **$P < 0.01$; ***$P < 0.001$; ****$P < 0.0001$ (repeated measures ANOVA followed by Tukey's adjusted comparisons of group means; IL-6 and CRP were $\log_{10}$ transformed to meet the distributional assumptions of the test).

[M8 (17)]. S-BMO was obtained from de-lactosed permeate, a dairy ingredient developed as a coproduct of whey protein isolation; deproteinization and removal of lactose was achieved by ultrafiltration and diafiltration (22). Mass spectrometry of the resulting oligosaccharide-enriched fraction established that it was composed primarily of 3′-sialyllactose and 6′-sialyllactose (88% of the oligosaccharide content), with the remaining structures consisting of neutral trihexoses of glucose, galactose, and *N*-acetylglucosamine-galactosamine and longer neutral oligosaccharides (see ref. 17). Given that sialyllactose is present in human milk, sialyllactose is the predominant oligosaccharide among the 15 structures identified in the S-BMO preparation, and S-BMO was obtained from a scalable source, this preparation provided an attractive starting point for our study.

S-BMO was added to the M8 diet at a level that approximated HMO levels in breastmilk (17). Five-week-old male germ-free C57BL6/J mice (n = 10 animals/treatment group in an initial experiment; n = 5/group in a repeat experiment; Fig. 2*A*) were monotonously fed either the unsupplemented M8 diet or M8 supplemented with S-BMO (both diets have comparable caloric density; 1.65 vs. 1.67 kcal/g, as defined by bomb calorimetry; ref. 17). The diets were begun 3 d before gavage with a defined consortium of bacterial strains cultured from a severely stunted 6-mo-old infant (LAZ, −3.48; ref. 17 and Dataset S1A). 16S rDNA sequence-based analysis of the infant's fecal microbiota had previously revealed that 78% of its bacterial composition (summed relative abundance of 97% identity Operational Taxonomic Units) was captured in this culture collection (17).

Community profiling by shotgun sequencing [COPRO-Seq (23)] of DNA prepared from cecal contents harvested from mice at the time of euthanasia 39 d postgavage (dpg), disclosed that consumption of S-BMO had no statistically significant effects on the representation of all but one low abundance member of the defined consortium (Dataset S1A). S-BMO supplementation resulted in significantly greater increases in total body weight, consistent with our earlier results (17). Quantitative magnetic resonance measurements performed on dpg 4 and dpg 38 disclosed that S-BMO administration produced significantly greater increases in lean body mass, and to a lesser extent fat mass, compared with control animals fed unsupplemented M8 (Fig. 2 *B–D*). Microcomputed tomography of femurs documented that S-BMO treatment produced statistically significant increases in trabecular bone volume (defined by bone volume normalized to tissue volume) and increased trabecular number (Fig. 2 *E* and *F*). Cortical bone thickness was also augmented, although this difference did not achieve statistical significance (P = 0.06, Mann–Whitney U test; Fig. 2*G*).

Analysis of serum samples obtained at the time of euthanasia revealed that consumption of the S-BMO-supplemented M8 diet produced a statistically significant reduction in circulating levels of CTX-I compared with the unsupplemented diet, but no significant differences in either serum P1NP or IGF1 (Fig. 2 *H–J* and Dataset S2). Staining tibial sections for tartrate-resistant alkaline phosphatase demonstrated a significant reduction in the number of osteoclasts per bone surface area, as well as reductions in total osteoclast number in S-BMO-treated mice (Fig. 2 *K–M*). Dynamic histomorphometry was performed by administering two dyes that are incorporated into growing bone (24): the first, calcein green, was given by i.p. injection 9 d before euthanasia; the second, alizarin red, was administered intraperitoneally 7 d later. The results revealed no significant effect of S-BMO on the rate of tibial bone formation per bone surface area, or on mineral apposition rate (Fig. 2 *N–P*). Serum levels of granulocyte-colony stimulating factor, which can induce apoptosis of mature osteoblasts, were not significantly different between the two treatment groups (Dataset S2). Together, these results suggest that that S-BMO treatment acts primarily to reduce bone resorption.

Mechanistic Studies of Osteoclastogenesis. We next measured serum levels of proteins known to regulate osteoclast differentiation and function. Receptor activator of nuclear factor-kappa B ligand (RANKL) induces osteoclast differentiation (25–27); it was significantly decreased in colonized animals receiving S-BMO (Fig. 3*A*). Osteoprotegerin opposes the activity of RANKL and blocks signaling through its cognate receptor, RANK, to decrease mature osteoclast formation (28, 29); Osteoprotegerin levels were significantly greater in the S-BMO-treated group (Fig. 3*B*). The decreased ratio of RANKL to osteoprotegerin suggested a shift away from a pro-osteoclastogenic environment; this conclusion is further supported by the observation that S-BMO-supplemented animals had significantly reduced serum levels of osteopontin, a mediator of osteoclast formation and function (30, 31) (Fig. 3*C*).

Myeloid lineage progenitors. Osteoclasts arise from myeloid cells, and can be formed by fusion of monocytes, macrophages, and their progenitors into multinucleated bone-resorbing cells (8) (Fig. 3*D*). Using flow cytometry (*SI Appendix*, *Supplementary Materials and Methods*), we identified alterations in myeloid lineage commitment within the bone marrow of S-BMO-treated mice; these include significant reductions in the representation of Lin^- IL-7Rα^- $cKit^+$ $Sca1^-$ $CD34^+$ $CD16/32^+$ granulocyte monocyte progenitors and Lin^- $CD115^+$ $cKit^+$ $Flt3^-$ $Ly6C^+$ $CD11b^-$ common monocyte progenitors (32, 33) (Fig. 3 *E* and *F* and Dataset S3A). Comparison of the two treatment groups also revealed that mice receiving S-BMO had significantly higher numbers of mature $CD115^+$ $cKit^-$ $Flt3^-$ $CD11b^+$ $Ly6C^+$ bone marrow monocytes (Fig. 3*G* and Dataset S3A), but no differences in the representation of other differentiated cell types in the myeloid lineage (eosinophils and neutrophils; Fig. 3 *H* and *I* and Dataset S3A). The effects of S-BMO supplementation were specific to the myeloid lineage; there were no statistically significant differences in the number of common lymphoid progenitors or megakaryocyte-erythroid progenitors between the two treatment groups (Dataset S3). Together, these findings support the notion that S-BMO supplementation promotes monocyte development at the expense of osteoclast formation.

Cytokines and chemokines linked to bone turnover. S-BMO did not significantly affect serum levels of IL-4 or IL-13, two Th2 cytokines known to negatively regulate osteoclast formation (Dataset S2). IL-6, which promotes osteoclast formation and can contribute to Th17-driven inflammation (34, 35), did not exhibit significant differences in its serum levels between the two treatment groups (Dataset S2). Transgenic mice that overexpress IL-5, an important eosinophil growth factor, show ectopic bone formation in their spleen (36). Although measurements of this serum cytokine did not disclose significant differences between the two groups of mice (Dataset S2), S-BMO produced a significant increase in serum eotaxin-1 (Fig. 4*A*). Eotaxin-1/CCL11 is chemotactic for Th2-associated eosinophils (37); its expression is regulated by NF-κB and can be induced by proinflammatory cytokines including IL-4, IL-13, IL-1α, and TNFα (38–40).

To further define the mechanism by which S-BMO decreases osteoclast formation and bone resorption, we investigated shifts in immune signaling and cellular composition within the intestine. Flow cytometry of colonic lamina propria cells (*SI Appendix*, *Supplementary Materials and Methods*) disclosed that mice fed the S-BMO-supplemented diet had significantly elevated levels of $CD45^+$ $CD11c^-$ $CD11b^+$ $SiglecF^+$ eosinophils (Fig. 4*B*), but not neutrophils or monocytes (Dataset S3). In keeping with the increased eosinophils, eotaxin-1 levels in cecal tissue were significantly higher in mice consuming S-BMO (Fig. 4*C*). IL-1α and IL-10 promote and decrease osteoclast differentiation, respectively, by influencing systemic levels of RANKL and osteoprotegerin (41, 42). Animals receiving S-BMO had significantly lower cecal tissue levels of proinflammatory IL-1α (Fig. 4*D*) and

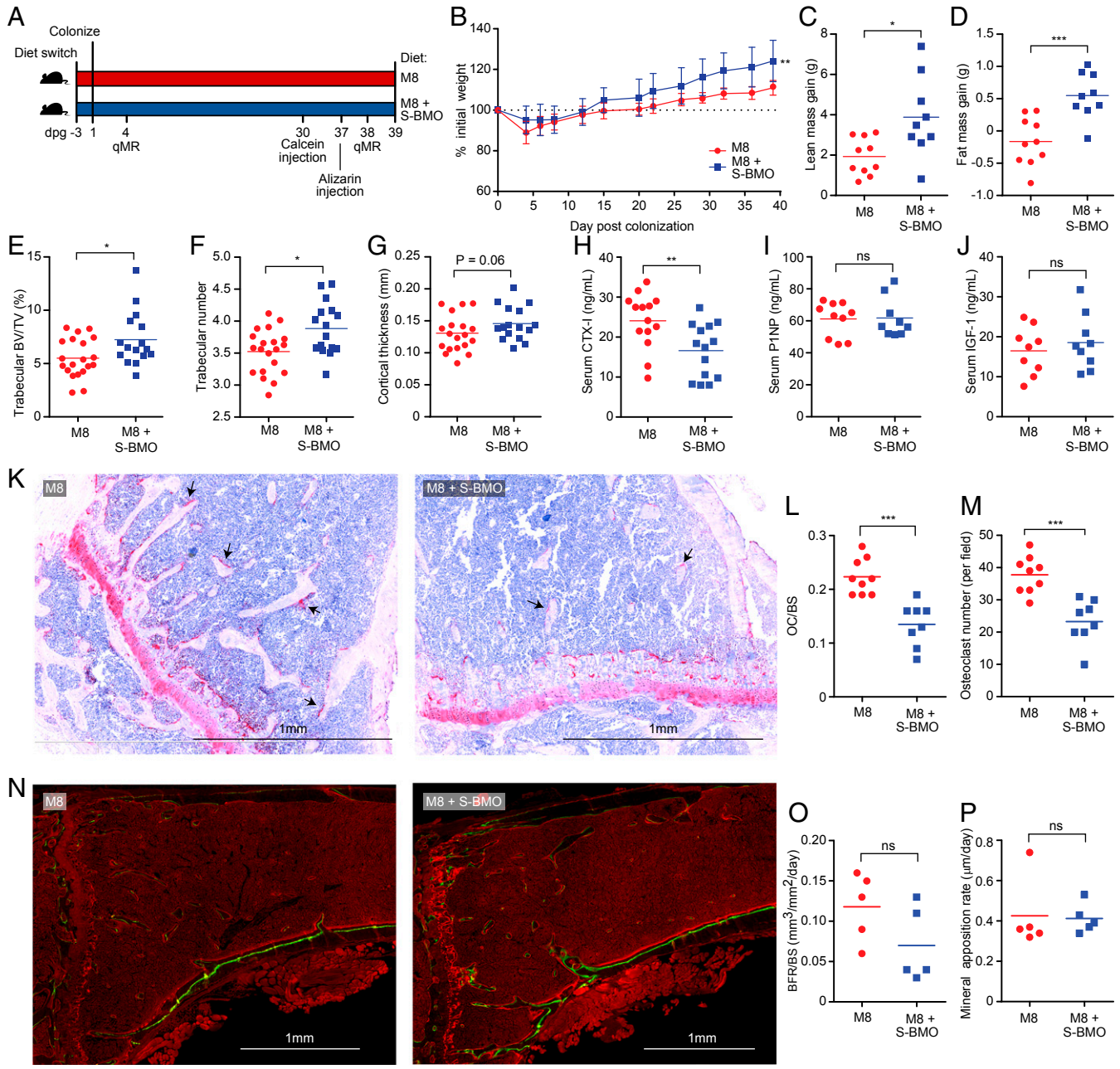

Fig. 2. S-BMO treatment reduces osteoclast number and decreases bone resorption, but does not affect osteoblast function in a gnotobiotic mouse model of infant undernutrition. (*A*) Study design. M8, representative Malawian diet. Note that serum samples were obtained at the time of euthanasia (dpg 39). (*B–D*) Effects of S-BMO treatment on weight, lean body mass, and fat mass gain (mean ± SD). (*E–G*) Microcomputed tomography of femoral bone showing effects of S-BMO on trabecular bone volume (*E*), number of trabeculae (*F*), and cortical bone thickness (*G*). (*H–J*) Serum samples taken on dpg 39 assayed for CTX-I, P1NP, and IGF1. (*K–M*) Effect of S-BMO on the representation of osteoclasts in tibial bone. Tartrate-resistant alkaline phosphatase staining of osteoclasts in bone sections reveals red multinucleated cells (e.g., black arrows in *K*). The number of osteoclasts per bone surface (OC/BS) (*L*) and osteoclast number per field (*M*) were quantified by tartrate-resistant alkaline phosphatase staining. (*N–P*) Dynamic histomorphometry of tibial bone (*N*) with results quantified as bone formation rate per bone surface (BFR/BS) (*O*) and mineral apposition rate (*P*). Each dot represents an individual animal. Horizontal lines in *C–J* and *L, M, O,* and *P* indicate mean values. ns, not significant; $*P < 0.05$; $**P < 0.01$; $***P < 0.001$ (Mann–Whitney *U* test).

trended toward having higher tissue levels of IL-10 compared with controls ($P = 0.056$; Fig. 4*E*).

T-cell responses are known to have important effects on osteoclast development; T regulatory cells can inhibit osteoclast formation via production of IL-10 (43, 44), whereas immune responses linked to the Th17 axis, including production of IL-17A and IL-23, can enhance osteoclast differentiation (9). The microbiota can, in turn, influence Th17 and T regulatory cell expansion (45, 46). We found no statistically significant differences in overall T-cell number, or in the number of $CD4^+$ T cells, $FoxP3^+$ T regulatory cells, or $IL\text{-}17^+$ Th17 cells in the colons of mice belonging to the two treatment groups (Dataset S3).

Intestinal gene expression. There is evidence from infants consuming breast milk that a small fraction of sialylated oligosaccharides may be absorbed in the small intestine (47). Therefore, we performed RNA-Seq, using RNA isolated from the distal third of the small intestines of mice in both treatment groups. An analysis of differential gene expression (DESeq2; see *SI Appendix, Supplementary*

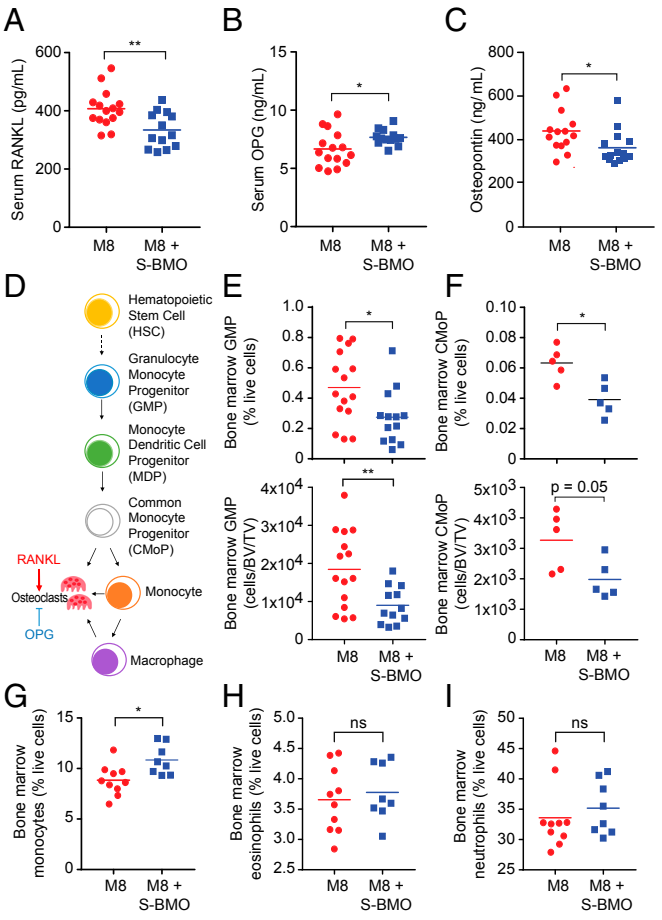

Fig. 3. Effects of S-BMO on osteoclastogenesis. (*A–C*) Serum levels of RANKL, osteoprotegerin (OPG), and osteopontin. (*D–F*) Bone marrow osteoclast progenitors enumerated via flow cytometry. Diagram of osteoclast differentiation (*D*). Numbers of granulocyte-monocyte progenitors [GMP; defined as Lineage (Lin)$^-$ IL-7Rα^- cKit$^+$ Sca1$^-$ CD34$^+$ CD16/32$^+$ cells; (*E*)] and common monocyte progenitors [CMoP; Lin$^-$ CD115$^+$ cKit$^+$ Flt3$^-$ Ly6C$^+$ CD11b$^-$ cells (*F*)]. See *Methods* for a list of Lineage markers. (*G–I*) Representation of bone marrow monocytes [CD115$^+$ cKit$^-$ Flt3$^-$ CD11b$^+$ Ly6C$^+$ cells (*G*)], eosinophils [CD45$^+$ CD11b$^+$ CD11c$^-$ SiglecF$^+$ cells (*H*)] and neutrophils [CD45$^+$ CD11b$^+$ CD11c$^-$ Ly6G$^+$ cells (*I*)]. Each dot in *A–C* and *E–I* indicates the value for an individual animal with horizontal lines representing mean values. ns, not significant; $*P < 0.05$; $**P < 0.01$ (Mann–Whitney *U* test).

Materials and Methods) identified 164 genes whose expression was significantly altered by the addition of S-BMO to the base diet (Fig. 4*F* and Dataset S4A). A comprehensive literature analysis was performed to identify relevant biological processes and pathways represented by the differentially expressed genes; this was accomplished with an automated Biological Knowledge Generation Engine that extracts all abstracts from PubMed that reference genes of interest (or their synonyms), using natural language processing and a biological language dictionary that is not restricted to fixed pathway and ontology knowledge bases. Conditional probability analysis calculated the statistical enrichment of biological concepts (processes/pathways) over those that occur by random sampling. Related concepts built from the list of differentially expressed genes were further clustered into higher-level themes (e.g., biological pathways/processes; see *SI Appendix, Supplementary Materials and Methods*).

A number of genes in the eosinophil theme exhibited significant differences in their expression in mice receiving S-BMO (Dataset S4B); they include increases in expression of *siglecF*, which encodes sialic acid binding Ig-like lectin F, a marker of gut eosinophils; *CD300lf*, which specifies a glycoprotein that augments IL-4- and IL-13-induced signaling, negatively regulates MyD88 and TRIF-dependent TLR signaling, and inhibits osteoclast formation (48–50); *Hck*, a regulator of innate immune responses that acts downstream of multiple cytokine receptors (IL-2, IL-6, IL-8) (51); and *Defb1*, a defensin reported to have a protective effect against the development of inflammatory bowel disease in humans (52). Moreover, *Dusp5*, a negative regulator of eosinophil survival and function, was suppressed (53) (Fig. 4*F*).

Small intestinal tuft cells. Tuft cells are chemosensory members of the gut epithelium derived from LGR5$^+$ crypt stem cells; they are distributed along the length of the gut and possess a distinctive cluster of microvilli at their apical surface. In addition, volume-rendering ultrastructural studies have disclosed an elaborate tubular network that includes cytospinules that connect tuft cells to the nuclei of neighboring epithelial cells (54). Their elaborate tubular connections to other epithelial cells, as well as to the gut lumen, allows tuft cells to serve as sentinels; one manifestation of this function is to orchestrate T-helper type 2 (Th2) immune responses to microbes (55, 56). A recent study showed that succinate, a product of bacterial fermentation, signals through the succinate receptor 1 (Sucnr1) and free fatty acid receptor 3 (Ffar3) on intestinal tuft cells to trigger a Th2 immune response that includes increases in eosinophils (57). S-BMO-treated mice had significantly higher levels of succinate in their cecal contents compared with animals fed the unsupplemented M8 diet (Fig. 4*G* and Dataset S5A). Moreover, expression of *Scnr1* and *Ffar3* were both significantly increased in S-BMO-treated mice (Fig. 4*F*), along with the small intestinal tuft cell markers *Gnat3* (guanine nucleotide binding protein G subunit alpha 3), *Trpm5* (transient receptor potential cation channel subfamily M member 5), and *Dclk1* (double cortin-like kinase 1) (Dataset S4). On the basis of these observations, we used an antibody to DCLK1 to stain sections obtained from the proximal, middle, and distal thirds of the small intestine for tuft cells (n = 5 animals/treatment group). The results revealed significant S-BMO-associated increases in the numbers of tuft cells along the length of the small intestine (Fig. 4 *H* and *I*).

Overall, these results demonstrate that in colonized mice, S-BMO supplementation of the diet produces (*i*) a reduction in osteoclasts and their bone marrow myeloid progenitors, but no demonstrable effect on osteoblasts, (*ii*) corresponding changes in regulators of osteoclastogenesis [i.e., a reduction in an inducer of osteoclast differentiation (RANKL) and an accompanying increase in an inhibitor of this process (osteoprotegerin)], and (*iii*) changes in chemokines, cytokines, and cells linked to Th2 responses [i.e., local (intestinal) and systemic (serum) levels of eotaxin-1, increases in colonic eosinophil number, plus tuft cell responses to succinate].

Comparing Germ-Free and Colonized Mice Fed S-BMO Versus 2′-FL. To examine the role of the gut microbiota in mediating the effects of S-BMO on bone biology, we compared groups of age-matched male germ-free and colonized mice that had been killed after monotonously consuming either the S-BMO-supplemented or unsupplemented M8 diet for 42 d (n = 5 animals/treatment group; Fig. 2*A*). We also characterized the specificity of the effects of S-BMO on bone biology. Rather than using LNT (lacto-*N*-tetraose) or LNnT (lacto-*N*-neotetraose) as a nondecorated HMO control that has *N*-acetylglucosamine, we added 2′-FL to the drinking water of separate groups of colonized and germ-free mice fed the base M8 diet (n = 5 mice/treatment group). This HMO is a major component of breast milk in secretor mothers who possess a functional *FUT2* gene (58) and is currently being added to some infant milk formulas.

Microbial community structure and metabolism. Supplementation with 2′-FL produced modest changes in cecal microbial community composition, with only two bacterial taxa (*Bifidobacterium catenulatum* and *Collinsella aerofaciens*) exhibiting significant

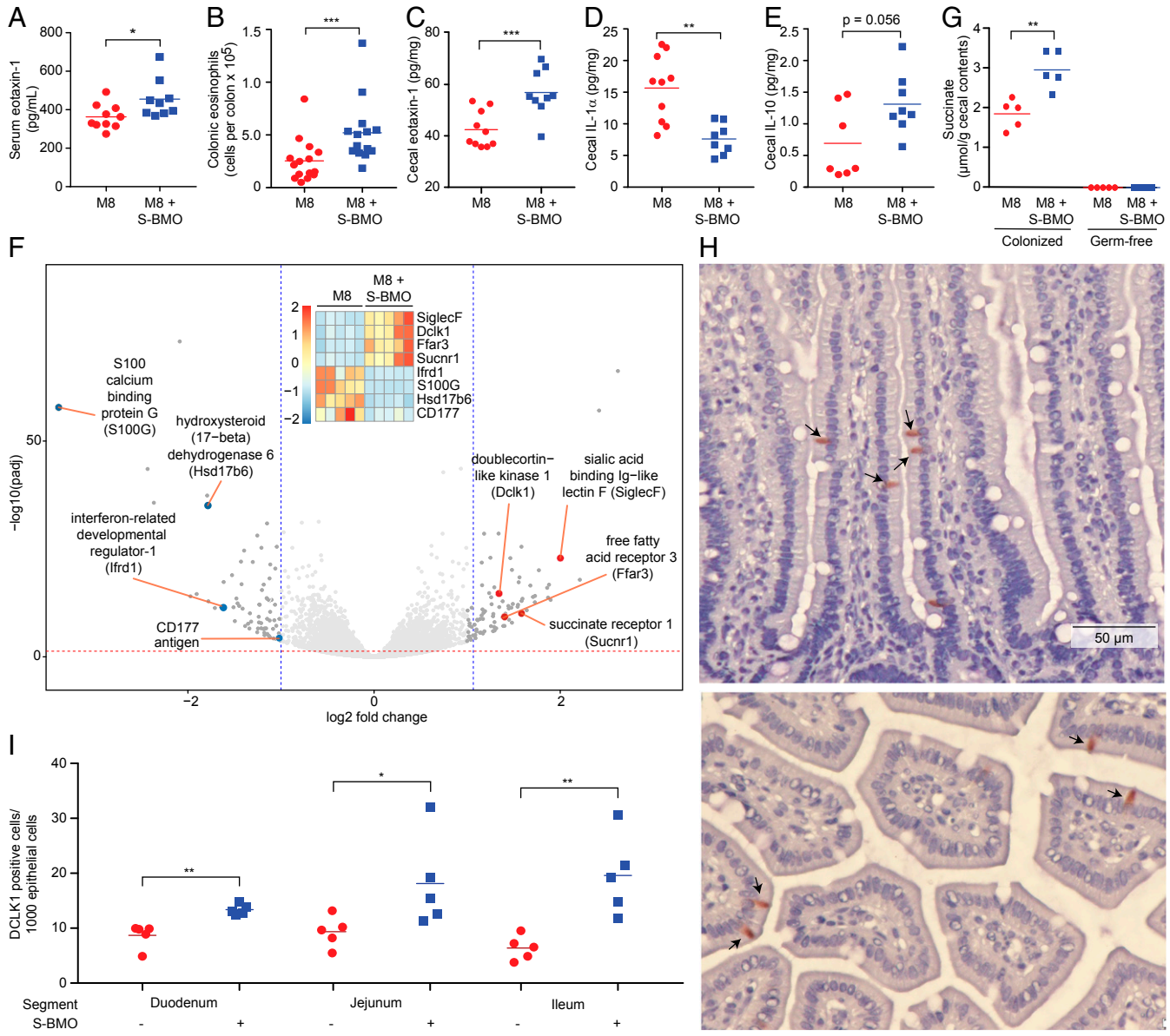

Fig. 4. Effects of S-BMO on immune function, intestinal gene expression, the representation of tuft cells, and metabolism. (*A*) Serum eotaxin levels defined at the time of euthanasia. (*B*) Quantifying colonic eosinophils ($CD45^+$ $CD11c^-$ $CD11b^+$ $SiglecF^+$) by flow cytometry. (*C*–*E*) Levels of eotaxin-1 (*C*), IL-1α (*D*), and IL-10 (*E*) in cecal tissue. (*F*) Volcano plot of host genes whose expression in the distal third of the small intestine was significantly affected by consumption of the S-BMO-supplemented diet. Differential expression was defined by DESeq2. (*Inset*) Shows selected genes associated with Th2-related responses involving tuft cells or eosinophils. The vertical colored scale bar in the *Inset* denotes relative expression. (*G*) Succinate levels in cecal contents harvested from colonized and germ-free mice fed the unsupplemented or S-BMO supplemented M8 diet. (*H* and *I*) Animals consuming the S-BMO-supplemented diet have significant increases in the number of $DCLK^+$ tuft cells (e.g., arrows in *H*) in the duodenum, jejunum, and ileum (*I*). The *Upper* and *Lower* subpanels in *H* show longitudinal and transverse sections of villi, respectively. Each dot in *A*, *E*, *G*, and *I* represents the value obtained for an individual animal; horizontal lines represent mean values $*P < 0.05$, $**P < 0.01$; $***P < 0.001$ (Mann–Whitney *U* test).

differences in their relative abundances; the representation of these organisms was not significantly affected by S-BMO (Dataset S1A). Targeted gas chromatography (GC)-mass spectrometry of cecal contents revealed that in this community context, the increase in succinate levels was specific to S-BMO-treated animals and was microbiota-dependent (Dataset S5).

The bacterial consortium introduced into mice contained a total of 29 genes encoding known or predicted sialidases and 30 fucosidases. The distribution of these genes in members of the defined community, and their assignments to different families of carbohydrate active enzymes, are described in Dataset S1B.

Nontargeted liquid chromatography-quadrupole time-of-flight mass spectrometry of cecal contents, harvested at the time of euthanasia from colonized and germ-free mice fed the M8 diet with or without S-BMO, revealed that the predominant product of bacterial S-BMO metabolism was *N*-acetyl-2,3-dehydro-2-deoxyneuraminic acid (*SI Appendix*, Fig. S1). This metabolite was not detected in the serum of S-BMO-treated colonized mice, nor in the ceca or serum of colonized mice fed the unsupplemented control diet or in germ-free mice fed either of the two diets (*SI Appendix*, Fig. S1). The biological effects of this compound are poorly defined, as are its interactions with Siglecs,

including SiglecF or Siglec15 [the latter regulates osteoclast differentiation through its modulation of RANKL signaling (59)]. Nonetheless, the absence of detectable serum levels of the metabolite suggests it is not involved in direct signaling from gut to bone.

Immune and bone phenotypes. In contrast to its effects in colonized mice, S-BMO administration to germ-free animals did not produce statistically significant effects on body weight (17.23 ± 0.95 g vs. 19.1 ± 0.27 g for controls; $P = 0.99$, Mann–Whitney U test) or alter femoral cortical bone thickness (0.11 ± 0.004 mm vs. 0.11± 0.003 mm for controls; $P = 0.15$, Mann–Whitney U test), or significantly affect serum levels of RANKL, IL-1α, or IL-10 (Dataset S2), nor did it decrease bone marrow granulocyte monocyte progenitors or affect the representation of bone marrow common monocyte progenitors and mature monocytes (Dataset S3). Unlike colonized mice fed S-BMO, colonic eosinophils were reduced rather than increased in germ-free mice (0.98 ± 0.24% vs. 3.28 ± 0.59% of live cells; $P < 0.05$, Mann–Whitney U test). However, S-BMO supplementation of the M8 diet was sufficient to increase trabecular volume in germ-free animals (8.57 ± 0.45% of total bone volume vs. 5.83 ± 0.41% for controls; $P < 0.05$, Mann–Whitney U test), increase serum osteoprotegerin, and decrease serum CTX-I (Dataset S2), suggesting that S-BMO can influence bone resorption, but requires the microbiota to exert its full effect on osteoclast lineage commitment and immune signaling. As there are small differences in micronutrient content between the two diets, including calcium and phosphorus which are higher in S-BMO-supplemented M8 (388 vs. 428 ppm and 1,143 vs. 1,291 ppm, respectively), we cannot exclude the possibility that these and/or other constituents of S-BMO contribute to the observed microbiota-independent effects.

In contrast to S-BMO supplementation, we did not observe statistically significant effects of 2′-FL supplementation on weight gain, femoral trabecular volume, cortical thickness, the number of bone marrow granulocyte monocyte progenitors, serum levels of CTX-I, and eotaxin-1 or cecal succinate levels in colonized mice (*SI Appendix*, Fig. S2 *A–F* and Dataset S5). However, unlike S-BMO, common monocyte progenitors and mature monocytes were significantly increased with 2′-FL administration (*SI Appendix*, Fig. S2 *G* and *H*), whereas colonic eosinophils were significantly decreased (*SI Appendix*, Fig. S2*I*). As with S-BMO, 2′-FL did not have significant effects on P1NP levels in colonized animals (Dataset S6).

Together, our results provide evidence of the specificity of S-BMO's effects on osteoclasts and their bone marrow progenitors, regulators of osteoclastogenesis, and chemokines and cytokines linked to Th2 responses. Moreover, they demonstrate that the bacterial community obtained from the stunted infant was required for the observed effects of S-BMO on cecal succinate levels, the decrease in RANKL, the concomitant decrease in osteoclast progenitors, and the colonic IL-1α, IL-10, and eosinophil responses.

Discussion

Our study has focused on the question of how interactions among milk glycans, the gut microbiota, and the immune system regulate bone growth. A corollary to this question is the degree to which persistent stunting in children with undernutrition reflects increased osteoclastic activity and/or diminished osteoblastic activity. Although the GH/IGF1 axis is central to linear growth via its actions on chondrocytes at the growth plate (60), there is a relative paucity of studies that have examined the association between biomarkers of bone turnover and growth faltering in early childhood. One report disclosed a marked increase in serum osteoprotegerin/RANKL ratios in neonates who were born short for gestational age compared with those with normal anthropometry, suggesting a potential compensatory response, mediated by elevated osteoprotegerin, to delayed neonatal growth (61). Furthermore, a systematic review and meta-analysis of the effects of breastfeeding promotion interventions failed to find significant changes in ponderal or linear growth (62), whereas a large prospective study in the Netherlands documented an association between breastfeeding and higher bone mass at 6 y of age (63). However, as breastmilk composition (including its oligosaccharides) varies between mothers, as well as over time within a given mother, the relationships between specific molecular components of breast milk and physiologic outcomes/biomarkers (such as linear growth/markers of bone turnover) are difficult to define in the absence of carefully designed and well-controlled longitudinal studies.

Previous preclinical studies of adult germ-free and conventionally raised mice have linked the microbiota to regulation of bone mass, although the effects reported are context-dependent, with sex and genetic background influencing observed phenotypes (e.g., refs. 64–66). Data about the effects of the microbiota on bone biology in younger animals are more limited. Studies of young, conventionally raised animals have shown that repeated courses of treatment with orally administered antibiotics during the first 40 postnatal days increase the rate of body mass gain and bone growth (67). *Lactobacillus rhamnosus* promoted bone building when introduced into young germ-free mice; the effect was associated with butyrate-induced increases in T regulatory cells (44). Young germ-free mice fed a nutritionally depleted diet, but not their conventionally raised counterparts, exhibited a growth hormone-resistant state manifest in part by reduced femoral length and body mass gain; the beneficial effect of a gut microbiota on the GH–IGF axis was recapitulated in undernourished germ-free mice by monocolonization with *Lactobacillus plantarum* (68), prompting the authors to emphasize the importance of advancing from these types of preclinical observations to an analysis of the role of the gut microbiota on bone growth/stunting children with undernutrition (69).

In this report, we describe a cohort of stunted Bangladeshi children with SAM who were studied before, during, and after completion of nutritional rehabilitation with therapeutic foods. The results reveal a significant reduction in plasma levels of a biomarker of osteoclastic activity (CTX-1) by the end of treatment. Although this reduction was sustained during the 6-mo period of follow-up, it was not accompanied by changes in osteoblastic activity, as assessed by plasma PN1P levels, nor was it associated with any improvement in their severe stunting, suggesting that this reduction in osteoclast number/activity is insufficient to ameliorate stunting without concomitant augmentation in osteoblastic function and/or other anabolic processes.

In follow-up mechanistic studies conducted in gnotobiotic mice, we provide evidence for a causal link between milk oligosaccharides and regulation of osteoclast formation and function. When administered to gnotobiotic mice colonized with a consortium of cultured bacterial strains from a 6-mo-old stunted infant, this purified preparation of sialylated oligosaccharides, recovered from normally discarded ingredients during the isolation of whey protein, produced a reduction in osteoclasts and their bone marrow myeloid progenitors without demonstrable effects on osteoblasts. Mechanistic studies disclosed changes in regulators of osteoclastogenesis, including a reduction in an inducer of osteoclast differentiation (RANKL), an increase in an inhibitor of this process (osteoprotegerin), plus alterations in chemokines, cytokines, and cells linked to Th2 responses. The interaction among S-BMO, the microbiota, and host distal small intestinal, cecal, and colonic cell populations was manifested by (*i*) decreased cecal tissue levels of a known promoter and increased levels of a known inhibitor of osteoclast differentiation (IL-1α and IL-10, respectively, which act through their effects on systemic levels of RANKL and osteoprotegerin), (*ii*) increases in cecal tissue levels of eotaxin-1 (chemotactic for Th2-associated eosinophils), (*iii*) increases in expression of the gene encoding a sialic acid binding Ig-like lectin F (SiglecF; a marker of gut eosinophils) and suppression of *Dusp5* (a negative regulator of eosinophil survival and function), (*iv*) S-BMO and microbiota-dependent increases in cecal levels of succinate, a product of

microbial fermentation, and (*v*) increased numbers of small intestinal tuft cells with accompanying changes in expression of tuft cell-associated genes indicative of activation of a signaling pathway that involves the succinate receptor 1 (Scnr1) and triggers a type 2 immune response leading to increases in the number of eosinophils. Evidence for the specificity for these effects comes from our finding that mice whose diets were supplemented with 2′-FL, a prominent fucosylated breast milk oligosaccharide, did not exhibit increases in trabecular bone volume, cortical thickness, the number of bone marrow osteoclast progenitors, changes in serum levels of CTX-I, or increases in eotaxin-1 and colonic eosinophils.

These observations raise a number of questions that need to be addressed in the future. The extent to which intestinal eosinophils and tuft cells contribute to S-BMO-associated reductions in osteoclast formation, number, and activity documented in this preclinical model remains to be deciphered. For example, what are the relative contributions of these cell lineages to the observed changes in effectors that regulate osteoclastogenesis? To what degree do tuft cell-based Th2 responses drive the gut eosinophil response? What are the cellular origins of the S-BMO-associated increase in eotaxin-1 in the gut and in peripheral blood? The lack of detectable protein in the S-BMO preparation suggests that the eosinophilia we document in the gut is not obviously related to the presence of this type of milk allergen (70). Although the S-BMO preparation is predominantly composed of sialyllactose, it contains other glycan components that could potentially contribute to the observed effects on the immune system and osteoclastogenesis. New synthetic approaches are now enabling production of other purified milk oligosaccharides at scale.

Our results with S-BMO and 2′-FL emphasize the need to test, in preclinical models, the effects of other purified oligosaccharide structures, singly at different doses and in different combinations, on bone growth as well as other facets of host physiology; the results should provide a more comprehensive understanding of the biological functions of human breast milk glycans and facilitate design of more effective therapeutic interventions for infants at risk for, or with already evident undernutrition (71). Advances in mass spectrometry have enabled the development of methods for rapid, absolute quantification of the numerous oligosaccharide structures present in breast milk (72). Our findings also provide a rationale for initiating studies of mothers and their offspring enrolled in birth cohorts in which consent/ethical approval has been obtained for serial collection of anthropometric data, breast milk, fecal samples, and plasma. Correlating results obtained from analyses of oligosaccharide structures present in breast milk, the biotransformation of these structures by the gut microbiota, microbiota development, and plasma biomarkers of bone development should provide new insights about interactions among HMOs, microbiota assembly/maturation, immune function, osteoclast and osteoblast development/activities, and linear growth.

Materials and Methods

Methods and protocols used for the study of children with SAM, colonization of gnotobiotic mice with a defined consortium of sequenced bacterial strains cultured from a stunted infant, quantification of the effects of S-BMO and 2′-FL on microbial community structure by short read shotgun sequencing of cecal DNA, GC-mass spectrometry and liquid chromatography-quadrupole time-of-flight mass spectrometry of metabolites present in cecal contents and serum, microcomputed tomography of bone, histochemical and dynamic histomorphometric analyses of bone, flow cytometry of bone marrow and cecal cell populations, RNA-Seq of distal small intestinal gene expression, histochemical and immunohistochemical analysis of intestinal sections, and measurement of cytokines, chemokines, and mediators of bone development and other proteins in serum and cecal tissue are described in *SI Appendix, Supplemental Materials and Methods*. The study of children with SAM was approved by the Ethical Review Committee at the International Centre for Diarrhoeal Disease Research, Bangladesh, and written informed consent was obtained from the parents or guardians of the study participants. Coded specimens and metadata were provided to Washington University under a materials transfer agreement (MTA) with approval from the Washington University institutional review board. Samples were stored at −80 °C in a dedicated biospecimen repository before analysis.

ACKNOWLEDGMENTS. We are grateful to the families of members enrolled in the human study for their participation and assistance. We are indebted to the staff and healthcare workers at the International Centre for Diarrhoeal Disease Research, Bangladesh, for their contributions to recruitment and enrollment of mothers as well as collection of biospecimens and data. We thank Dave O'Donnell, Maria Karlsson, Justin Serugo, Marty Meier, Sabrina Wagoner, and J. Hoisington-López for superb technical assistance, Kazi Ahsan for his contributions to maintaining the human biospecimen repository and associated database, Daniel Leib for his input regarding processing microcomputed tomography scan datasets from bone, and Vincent Lombard and Bernard Henrissat (Centre National de la Recherche Scientifique and Aix-Marseille Université) for their assistance with CAZyme annotations. This work was supported by the Bill & Melinda Gates Foundation plus NIH Grants DK30292 and AT008759. Microcomputed tomography, plus sectioning and histochemical staining of bone were performed using resources provided by the Washington University Musculoskeletal Research Center (NIH P30 AR057235). Glycosyn LLC generously supplied 2′-FL. C.A.C. received support from an NIH T32 training Grant (AI007172-38). J.I.G. is the recipient of a Thought Leader Award from Agilent Technologies.

1. Black RE, et al.; Maternal and Child Nutrition Study Group (2013) Maternal and child undernutrition and overweight in low-income and middle-income countries. *Lancet* 382:427–451.
2. Bhutta ZA, et al.; Lancet Nutrition Interventions Review Group, the Maternal and Child Nutrition Study Group (2013) Evidence-based interventions for improvement of maternal and child nutrition: What can be done and at what cost? *Lancet* 382:452–477.
3. Victora CG, et al.; Maternal and Child Undernutrition Study Group (2008) Maternal and child undernutrition: Consequences for adult health and human capital. *Lancet* 371:340–357.
4. Saleem AF, et al. (2015) Immunogenicity of poliovirus vaccines in chronically malnourished infants: A randomized controlled trial in Pakistan. *Vaccine* 33:2757–2763.
5. Millward DJ (2017) Nutrition, infection and stunting: The roles of deficiencies of individual nutrients and foods, and of inflammation, as determinants of reduced linear growth of children. *Nutr Res Rev* 30:50–72.
6. Syed S, et al. (2018) Biomarkers of systemic inflammation and growth in early infancy are associated with stunting in young Tanzanian children. *Nutrients* 10:1158.
7. DeBoer MD, et al. (2017) Systemic inflammation, growth factors, and linear growth in the setting of infection and malnutrition. *Nutrition* 33:248–253.
8. Novack DV, Mbalaviele G (2016) Osteoclasts–Key players in skeletal health and disease. *Microbiol Spectr* 4:MCHD-0011-2015.
9. Takayanagi H (2007) Osteoimmunology: Shared mechanisms and crosstalk between the immune and bone systems. *Nat Rev Immunol* 7:292–304.
10. Taichman RS (2005) Blood and bone: Two tissues whose fates are intertwined to create the hematopoietic stem-cell niche. *Blood* 105:2631–2639.
11. Ahmed SF, Farquharson C (2010) The effect of GH and IGF1 on linear growth and skeletal development and their modulation by SOCS proteins. *J Endocrinol* 206:249–259.
12. Kaneshiro S, et al. (2014) IL-6 negatively regulates osteoblast differentiation through the SHP2/MEK2 and SHP2/Akt2 pathways in vitro. *J Bone Miner Metab* 32:378–392.
13. Gasparetto M, Guariso G (2014) Crohn's disease and growth deficiency in children and adolescents. *World J Gastroenterol* 20:13219–13233.
14. Wong SC, Macrae VE, McGrogan P, Ahmed SF (2006) The role of pro-inflammatory cytokines in inflammatory bowel disease growth retardation. *J Pediatr Gastroenterol Nutr* 43:144–155.
15. Ballinger AB, Azooz O, El-Haj T, Poole S, Farthing MJG (2000) Growth failure occurs through a decrease in insulin-like growth factor 1 which is independent of undernutrition in a rat model of colitis. *Gut* 46:694–700.
16. Hokken-Koelega ACS, et al. (1991) Placebo-controlled, double-blind, cross-over trial of growth hormone treatment in prepubertal children with chronic renal failure. *Lancet* 338:585–590.
17. Charbonneau MR, et al. (2016) Sialylated milk oligosaccharides promote microbiota-dependent growth in models of infant undernutrition. *Cell* 164:859–871.
18. Ahmed T, et al. (1999) Mortality in severely malnourished children with diarrhoea and use of a standardised management protocol. *Lancet* 353:1919–1922.
19. Chubb SAP (2012) Measurement of C-terminal telopeptide of type I collagen (CTX) in serum. *Clin Biochem* 45:928–935.
20. Yokota K, et al. (2014) Combination of tumor necrosis factor α and interleukin-6 induces mouse osteoclast-like cells with bone resorption activity both in vitro and in vivo. *Arthritis Rheumatol* 66:121–129.
21. Amarasekara DS, et al. (2018) Regulation of osteoclast differentiation by cytokine networks. *Immune Netw* 18:e8.
22. Smith ST, Metzger L, Drake MA (2016) Evaluation of whey, milk, and delactosed permeates as salt substitutes. *J Dairy Sci* 99:8687–8698.

23. McNulty NP, et al. (2011) The impact of a consortium of fermented milk strains on the gut microbiome of gnotobiotic mice and monozygotic twins. *Sci Transl Med* 3:106ra106.
24. Schmidt IU, Dobnig H, Turner RT (1995) Intermittent parathyroid hormone treatment increases osteoblast number, steady state messenger ribonucleic acid levels for osteocalcin, and bone formation in tibial metaphysis of hypophysectomized female rats. *Endocrinology* 136:5127–5134.
25. Lacey DL, et al. (1998) Osteoprotegerin ligand is a cytokine that regulates osteoclast differentiation and activation. *Cell* 93:165–176.
26. Fuller K, Wong B, Fox S, Choi Y, Chambers TJ (1998) TRANCE is necessary and sufficient for osteoblast-mediated activation of bone resorption in osteoclasts. *J Exp Med* 188:997–1001.
27. Kong YY, et al. (1999) OPGL is a key regulator of osteoclastogenesis, lymphocyte development and lymph-node organogenesis. *Nature* 397:315–323.
28. Simonet WS, et al. (1997) Osteoprotegerin: A novel secreted protein involved in the regulation of bone density. *Cell* 89:309–319.
29. Yasuda H, et al. (1998) Identity of osteoclastogenesis inhibitory factor (OCIF) and osteoprotegerin (OPG): A mechanism by which OPG/OCIF inhibits osteoclastogenesis in vitro. *Endocrinology* 139:1329–1337.
30. Ge Q, et al. (2017) Osteopontin regulates macrophage activation and osteoclast formation in hypertensive patients with vascular calcification. *Sci Rep* 7:40253.
31. Reinholt FP, Hultenby K, Oldberg A, Heinegård D (1990) Osteopontin–A possible anchor of osteoclasts to bone. *Proc Natl Acad Sci USA* 87:4473–4475.
32. Challen GA, Boles N, Lin KK-Y, Goodell MA (2009) Mouse hematopoietic stem cell identification and analysis. *Cytometry A* 75:14–24.
33. Hettinger J, et al. (2013) Origin of monocytes and macrophages in a committed progenitor. *Nat Immunol* 14:821–830.
34. Axmann R, et al. (2009) Inhibition of interleukin-6 receptor directly blocks osteoclast formation in vitro and in vivo. *Arthritis Rheum* 60:2747–2756.
35. Kimura A, Kishimoto T (2010) IL-6: Regulator of Treg/Th17 balance. *Eur J Immunol* 40: 1830–1835.
36. Macias MP, et al. (2001) Expression of IL-5 alters bone metabolism and induces ossification of the spleen in transgenic mice. *J Clin Invest* 107:949–959.
37. Kitaura M, et al. (1996) Molecular cloning of human eotaxin, an eosinophil-selective CC chemokine, and identification of a specific eosinophil eotaxin receptor, CC chemokine receptor 3. *J Biol Chem* 271:7725–7730.
38. Matsukura S, et al. (1999) Activation of eotaxin gene transcription by NF-kappa B and STAT6 in human airway epithelial cells. *J Immunol* 163:6876–6883.
39. Hirst SJ, Hallsworth MP, Peng Q, Lee TH (2002) Selective induction of eotaxin release by interleukin-13 or interleukin-4 in human airway smooth muscle cells is synergistic with interleukin-1β and is mediated by the interleukin-4 receptor α-chain. *Am J Respir Crit Care Med* 165:1161–1171.
40. Neilsen CV, Bryce PJ (2010) Interleukin-13 directly promotes oesophagus production of CCL11 and CCL24 and the migration of eosinophils. *Clin Exp Allergy* 40:427–434.
41. Braun T, Zwerina J (2011) Positive regulators of osteoclastogenesis and bone resorption in rheumatoid arthritis. *Arthritis Res Ther* 13:235.
42. Kim JH, et al. (2009) The mechanism of osteoclast differentiation induced by IL-1. *J Immunol* 183:1862–1870.
43. Kim YG, et al. (2007) Human CD4+CD25+ regulatory T cells inhibit the differentiation of osteoclasts from peripheral blood mononuclear cells. *Biochem Biophys Res Commun* 357:1046–1052.
44. Tyagi AM, et al. (2018) The microbial metabolite butyrate stimulates bone formation via T regulatory cell-mediated regulation of WNT10B expression. *Immunity* 49:1116–1131.e7.
45. Ivanov II, et al. (2008) Specific microbiota direct the differentiation of IL-17-producing T-helper cells in the mucosa of the small intestine. *Cell Host Microbe* 4:337–349.
46. Atarashi K, et al. (2013) Treg induction by a rationally selected mixture of Clostridia strains from the human microbiota. *Nature* 500:232–236.
47. Ruhaak LR, Stroble C, Underwood MA, Lebrilla CB (2014) Detection of milk oligosaccharides in plasma of infants. *Anal Bioanal Chem* 406:5775–5784.
48. Moshkovits I, et al. (2015) CD300f associates with IL-4 receptor α and amplifies IL-4-induced immune cell responses. *Proc Natl Acad Sci USA* 112:8708–8713.
49. Lee S-M, Kim E-J, Suk K, Lee W-H (2011) CD300F blocks both MyD88 and TRIF-mediated TLR signaling through activation of Src homology region 2 domain-containing phosphatase 1. *J Immunol* 186:6296–6303.
50. Chung D-H, et al. (2003) CMRF-35-like molecule-1, a novel mouse myeloid receptor, can inhibit osteoclast formation. *J Immunol* 171:6541–6548.
51. Poh AR, O'Donoghue RJJ, Ernst M (2015) Hematopoietic cell kinase (HCK) as a therapeutic target in immune and cancer cells. *Oncotarget* 6:15752–15771.
52. Peyrin-Biroulet L, et al. (2010) Peroxisome proliferator-activated receptor gamma activation is required for maintenance of innate antimicrobial immunity in the colon. *Proc Natl Acad Sci USA* 107:8772–8777.
53. Holmes DA, Yeh J-H, Yan D, Xu M, Chan AC (2015) Dusp5 negatively regulates IL-33-mediated eosinophil survival and function. *EMBO J* 34:218–235.
54. Hoover B, et al. (2017) The intestinal tuft cell nanostructure in 3D. *Sci Rep* 7:1652.
55. Gerbe F, et al. (2011) Distinct ATOH1 and Neurog3 requirements define tuft cells as a new secretory cell type in the intestinal epithelium. *J Cell Biol* 192:767–780.
56. Howitt MR, et al. (2016) Tuft cells, taste-chemosensory cells, orchestrate parasite type 2 immunity in the gut. *Science* 351:1329–1333.
57. Nadjsombati MS, et al. (2018) Detection of succinate by intestinal tuft cells triggers a type 2 innate immune circuit. *Immunity* 49:33–41.e7.
58. Castanys-Muñoz E, Martin MJ, Prieto PA (2013) 2′-fucosyllactose: An abundant, genetically determined soluble glycan present in human milk. *Nutr Rev* 71:773–789.
59. Kameda Y, et al. (2015) Siglec-15 is a potential therapeutic target for postmenopausal osteoporosis. *Bone* 71:217–226.
60. Yakar S, Isaksson O (2016) Regulation of skeletal growth and mineral acquisition by the GH/IGF-1 axis: Lessons from mouse models. *Growth Horm IGF Res* 28:26–42.
61. Tenta R, et al. (2013) Bone metabolism compensates for the delayed growth in small for gestational age neonates. *Organogenesis* 9:55–59.
62. Giugliani ER, Horta BL, Loret de Mola C, Lisboa BO, Victora CG (2015) Effect of breastfeeding promotion interventions on child growth: A systematic review and meta-analysis. *Acta Paediatr* 104:20–29.
63. van den Hooven EH, et al. (2016) Associations of breast-feeding patterns and introduction of solid foods with childhood bone mass: The Generation R Study. *Br J Nutr* 115:1024–1032.
64. Sjögren K, et al. (2012) The gut microbiota regulates bone mass in mice. *J Bone Miner Res* 27:1357–1367.
65. Yan J, et al. (2016) Gut microbiota induce IGF-1 and promote bone formation and growth. *Proc Natl Acad Sci USA* 113:E7554–E7563.
66. Li J-Y, et al. (2016) Sex steroid deficiency-associated bone loss is microbiota dependent and prevented by probiotics. *J Clin Invest* 126:2049–2063.
67. Nobel YR, et al. (2015) Metabolic and metagenomic outcomes from early-life pulsed antibiotic treatment. *Nat Commun* 6:7486.
68. Schwarzer M, et al. (2016) Lactobacillus plantarum strain maintains growth of infant mice during chronic undernutrition. *Science* 351:854–857.
69. Poinsot P, Schwarzer M, Peretti N, Leulier F (2018) The emerging connections between IGF1, the intestinal microbiome, *Lactobacillus* strains and bone growth. *J Mol Endocrinol* 61:T103–T113.
70. Boettcher E, Crowe SE (2013) Dietary proteins and functional gastrointestinal disorders. *Am J Gastroenterol* 108:728–736.
71. Ahmed T, et al. (2014) Development and acceptability testing of ready-to-use supplementary food made from locally available food ingredients in Bangladesh. *BMC Pediatr* 14:164.
72. Xu G, et al. (2017) Absolute quantitation of human milk oligosaccharides reveals phenotypic variations during lactation. *J Nutr* 147:117–124.